MODELLING OF FATIGUE BEHAVIOUR OF A Cr-Mo STEEL DESIGNED FOR USAGE IN HYDROGEN FUEL CELL SYSTEMS

Rozina YORDANOVA, Tsvetelina LAZAROVA, Donka ANGELOVA, Alexander GEORGIEV

University of Chemical Technology and Metallurgy, Sofia, Bulgaria, EU, r.yordanova@uctm.edu

Abstract

Fatigue in Cr-Mo steel, JIS SCM435, candidate for use in fuel cell vehicles is investigated at different test frequencies in two groups of hydrogen charged and uncharged specimens under tension-compression fatigue and stress ratio $R = -1$. Specimens are machined in hour-glass shape with artificial hole from which initial cracks start their propagation.

The obtained fatigue data of each frequency are presented in plots “Crack length - Number of cycles” and “Fatigue crack growth rate - Crack length”. A mathematical model consists of double-parabolic-linear-curve is found for the data in the presentation “Fatigue crack growth rate - Crack length” and a comparison made between those curves for the different frequencies. The adequacy of modelling is checked and proved by comparison between experimental fatigue lifetimes and the calculated by the model.

Keywords: Fatigue, hydrogen fuel cell systems, Cr-Mo steel, short fatigue crack, crack growth rate

1. INTRODUCTION

Worldwide there are many investigations on one of most attractive alternative energy technologies, the hydrogen technology including hydrogen produce, and hydrogen storage and infrastructure. The main experimental results of these studies are summarized in the scheme shown in **Fig. 1**, which presents the main hydrogen technology applications. The scheme has been called "Hydrogen Economy of the Future" and its author is the well-known Prof. Murakami, the Director of the Japanese Institute for hydrogen-economy research and development, HYDROGENIUS, at Kyushu University, Japan [1].

Based on the research related to application of hydrogen technology various types of fuel cells for electricity produce are constructed. In the recent years an intense development of automotive fuel cell technology led to usage of certain number of hydrogen vehicles in most big cities across the world.

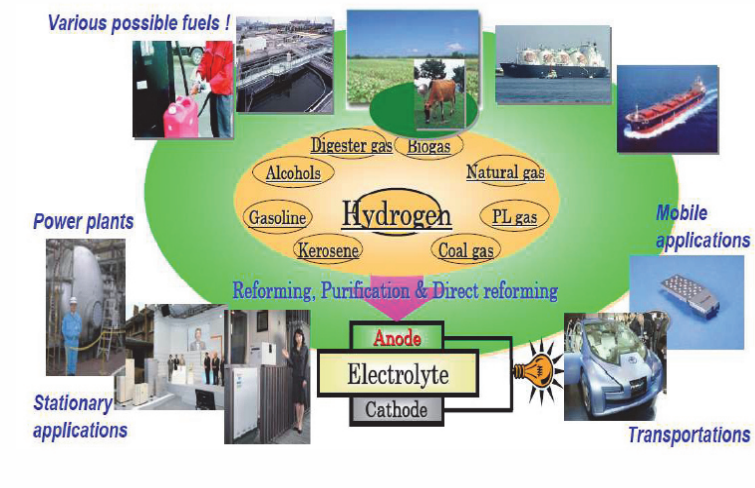

Fig. 1 "Hydrogen Economy of the Future"

2. MATERIAL AND EXPERIMENTAL WORK AFTER MURAKAMI

In this work data of fatigue crack propagation in Cr - Mo steel JIS SCM435 published by Murakami were used [1-3].

2.1 Material and specimens

The material investigated by Murakami is a Cr - Mo steel JIS SCM435, [1-3] used for hydrogen infrastructure - hydrogen accumulator. The hydrogen content of SCM435 steel decreases with time after charging. This suggests that the hydrogen content in specimens also decreases during fatigue testing. The hydrogen content before and after a fatigue test was always checked [1,3]. Chemical composition and the Vickers hardness are shown in **Table 1**.

Table 1 Chemical composition and Vickers hardness of Steel SCM 435

Chemical composition (wt. %)										Vickers hardness *HV*
C	Si	Mn	P	S	Cr	Ni	Cu	Mo	H+	
0.37	0.18	0.78	0.025	0.015	1.05	0.09	0.1	0.15	~0	330

Murakami investigated the influence of hydrogen on Steel 435 using two types of specimens: uncharged and hydrogen charged ones; hydrogen was artificially charged soaking them in a 20% ammonium thiocyanate solution (NH4 SCN). Tension - compression fatigue test was carried out by using both types of specimens.

Figs. 2a and b show the fatigue specimen geometry and dimensions and the dimensions of the small hole which was introduced into the specimen surface. After polishing with #2000 emery paper, the specimen surface was finished by buffing using colloidal SiO_2 (0.04 μm) solution. In the hydrogen-charged specimens, the specimen surface was buffed after hydrogen charging, and the hole was then introduced immediately.

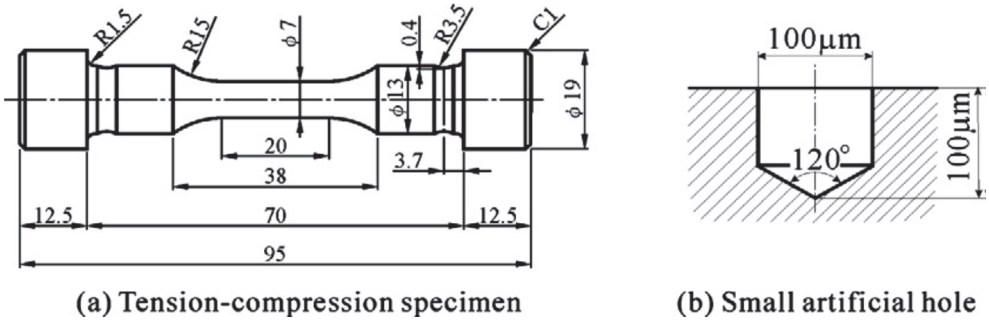

(a) Tension-compression specimen (b) Small artificial hole

Fig. 2 Geometry and dimensions of fatigue test specimens, in mm

2.2 Method of hydrogen charging

Hydrogen was charged into the specimens of SCM 435 by soaking them in a 20% ammonium thiocyanate solution (NH4 SCN), [1, 4]. The charging time is 24 h and the temperature of solution is 50 ◦C. Hydrogen content of Uncharged specimen is 0.26 ppm and for hydrogen-charged ones are 10 ppm (1.5 h after hydrogen charging).

2.3 Method of fatigue testing

Fatigue tests of the hydrogen-charged and uncharged specimens were carried out at room temperature in laboratory air. The tension compression-fatigue tests for SCM435 were conducted at a stress ratio R = - 1 and at a testing frequency between 0.2 Hz and 20 Hz [1-3].

3. METHODS FOR ANALYSIS

3.1 Replication technique

Surface tracking method for short fatigue crack growth consists of making a replica (stamp) of the specimen's surface and subsequent monitoring of crack length and its propagation [1-6]. Replicas are taken into two mutually opposite surfaces of the specimen, which ensures full coverage of the working area of the specimen. At the beginning making of replicas and their examination is at certain number of cycles until the discovering of a crack, after that the interval is reduced significantly.

3.2 Modelling of fatigue behaviour

Crack growth rate *da/dN* [μm/cycle] is determined as a ratio of differences between whole length of the crack *a,* μm and *N* (cycles) [4].

For all data presentations we use parabolic-linear mathematical model "Crack growth rate, *da/dN* - crack length *a*" at cyclic tension - compression loading - Eq. (1) - based on some investigations made in [5, 6]. The model comprises description of fatigue crack growth behaviour in its three different stages (I. Stage of short fatigue crack growth (SFC), II. Stage of physically small fatigue crack growth (PhSFC), III, stage of long fatigue crack growth (LFC)) and analytical determination of the characteristics dividing those three stages and known as microstructural barriers d_1 and d_2, at which cracks are slowing down and stop; the other model parameters include a_0 and a_f - the initial and final crack sizes, and D_i -material constants.

$$\mathbf{M(a):}\begin{cases} SFC:\left(\frac{da}{dN}\right)_{sh} = D_1 a^2 + D_2 a + D_3;\ a \in [a_0,\ d_1] \\ PhSFC:\left(\frac{da}{dN}\right)_{phs} = D_4 a^2 + D_5 a + D_6;\ a \in [d_1,\ d_2] \\ LCF:\left(\frac{da}{dN}\right)_{l} = D_7 a^{D_8};\quad a \geq d_2 \end{cases} \tag{1}$$

During the stage I fatigue cracks initiate and propagate as shear cracks - MODE II. Entering into the stage II the shear fatigue cracks change into tensile cracks - MODE I. During these two stages fatigue cracks are strongly influenced by different elements of metal microstructure, and their propagation can be described by parabolic functions. The III stage shows that metal microstructure does not influence fatigue crack growth and fatigue crack propagates with increasing rate up to the complete failure of specimen [7, 8].

4. RESULTS AND DISCUSSION

Fig. 3 shows the relationship between crack length *a* and number of cycle *N* under the tenshon-compression stress amplitude σ_a = 600 MPa, frequency *f* = 0.2, 2 and 20 Hz.

Murakami observes [3] that the crack of the hydrogen-charged specimen looks thinner than the uncharged specimens. The crack paths of the hydrogen-charged specimens tested under *f* = 0.2 and 2 Hz are relatively more linear than those of the uncharged specimens and also that of the hydrogen-charged specimen tested under *f* = 20 Hz. The crack tip of the uncharged specimen has many slip bands spreaded broad beside the crack line. The crack growth rates under hydrogen effect are 30 times higher than those for uncharged specimens. The slip bands of the hydrogen-charged specimens were localized only at very narrow area beside the crack line. These characteristics are commonly observed in hydrogen-charged specimens of other materials [3].

In our work we did proceed fatigue data of Murakami using the proposed model in Eq. (1). The values of all coefficients calculated by the model are shown in **Table 2**.

Crack length, microstructural barriers at different frequency of fatigue loading and fatigue lifetimes calculated by the model are shown in **Table 3**.

The proposed model is supported by the comparison of the fatigue lifetime predicted by Eq. (2), $N_{f,mod}$, and the actual fatigue lifetime, $N_{f,exp}$, both presented in **Table 3**:

$$N_{f,\mathrm{mod}} = N_0 + \int_{a_0}^{d_1} \frac{1}{\left(D_1 a^2 + D_2 a + D_3\right)} da + \int_{d_1}^{d_2} \frac{1}{\left(D_4 a^2 + D_5 a + D_6\right)} da + \int_{d_2}^{a_f} \frac{1}{D_7 . a^{D_8}} da \,, \tag{2}$$

where N_0 is the number of cycles for crack initiation.

To estimate the applicability of the model, a comparison is made between $N_{f,mod}$ and $N_{f,exp}$, Eq. (3), **Table 3**.

$$S = 100(N_{f,\exp} - N_{f,\mathrm{mod}}) / N_{f,\exp} \tag{3}$$

The graphical presentation of the model *da/dN-a* from Eq. (1) can be seen in **Fig. 3** for steel SCM 435. Mathematical modelling of experimental data of hydrogen-charged specimens under different frequency, 0.2, 2 and 20 Hz is shown in **Fig. 4**. Comparison between hydrogen - charged and uncharged specimens tested at f = 20 Hz is shown in **Fig. 4c**. The comparative analysis of the presentations shown that hydrogen charged specimens increasing their fatigue crack growth compared with those for uncharged specimens, resulting in a shorter fatigue life $N_{f,exp}$, (**Table 3**).

On the basis of comparative analysis of the models describing the behaviour of short fatigue crack, the influence of the frequency at the cyclic loading on the test specimens which are hydrogen-charged is revealed. The fatigue crack growth rate *da/dN* of the hydrogen charged specimens is much higher than that of uncharged specimens, **Fig. 5**. The decrease in frequency leads to a shift of microstructural barriers d_1 and d_2 at the left in the same graph; also to an increase of crack growth rates.

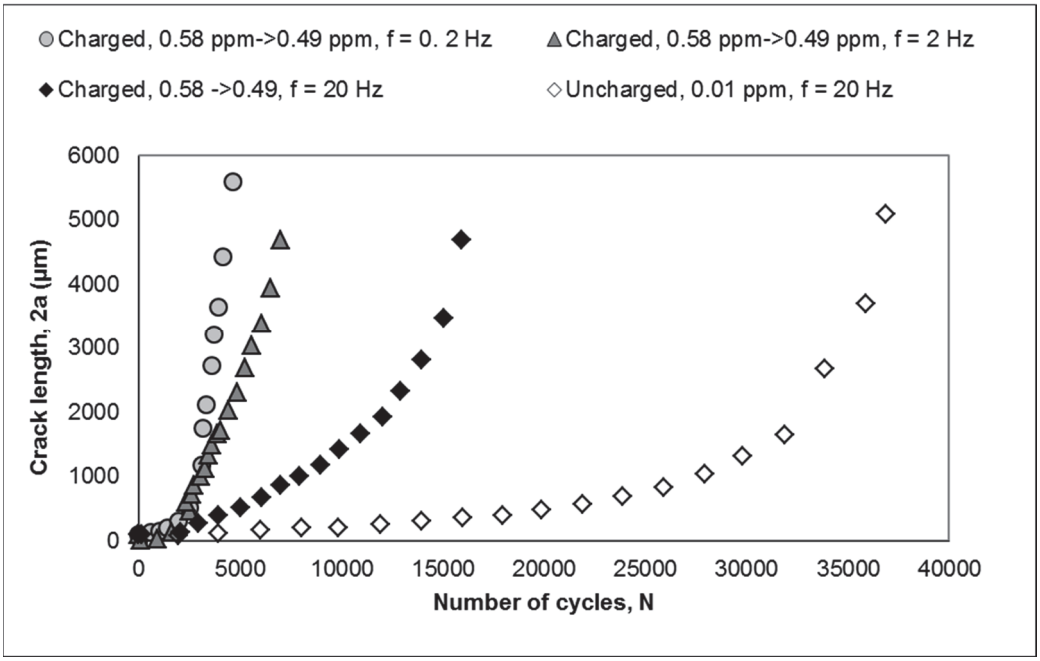

Fig. 3 Dependence "Crack length, *a* - number of cycles, *N*" at σ_a = 600 MPa

Table 2 Coefficients D_i at different frequency of fatigue loading

specimens	f (Hz	I stage (SFC)			II stage (PhSFC)			III stage (LFC)	
		D_1	D_2	D_3	D_1	D_2	D_3	D_1	D_2
Charged	0.2	-1.08×10^{-6}	19.8×10^{-4}	-18.4×10^{-2}	-1.71×10^{-6}	99.2×10^{-4}	-11.9	8.10^{-8}	2.091
	2	-1.72×10^{-5}	28.2×10^{-2}	-9.8×10^{-2}	-3.47×10^{-6}	10.3×10^{-3}	-6.38	9.6×10^{-5}	1.152
	20	-6.43×10^{-6}	19.9×10^{-4}	25.2×10^{-2}	-8.78×10^{-7}	1.37×10^{-7}	-34×10^{-2}	5.7×10^{-5}	1.123
Uncharged	20	-2.22×10^{-7}	2.32×10^{-4}	-2.70×10^{-2}	-8.60×10^{-7}	3.25×10^{-4}	-14×10^{-2}	2.6×10^{-7}	1.801

Table 3 Crack lengths, microstructural barriers, fatigue lifetimes with corresponding errors S

specimens	f (Hz)	a_0 (μm)	N_0 (cycles)	a_f (μm)	d_1 (μm)	d_2 (μm)	$N_{f,mod}$ (cycles)	$N_{f,exp}$ (cycles)	S (%)
Charged	0.2	435	2314	5589	1682	3581	5589	4487	-24.5
	2	488	2323	4666	1084	20071	7384	6979	-5.8
	20	163	3908	5163	596	1676	34100	36955	7.7
Uncharged	20	115	2180	1912	377	997	13234	12073	-9.6

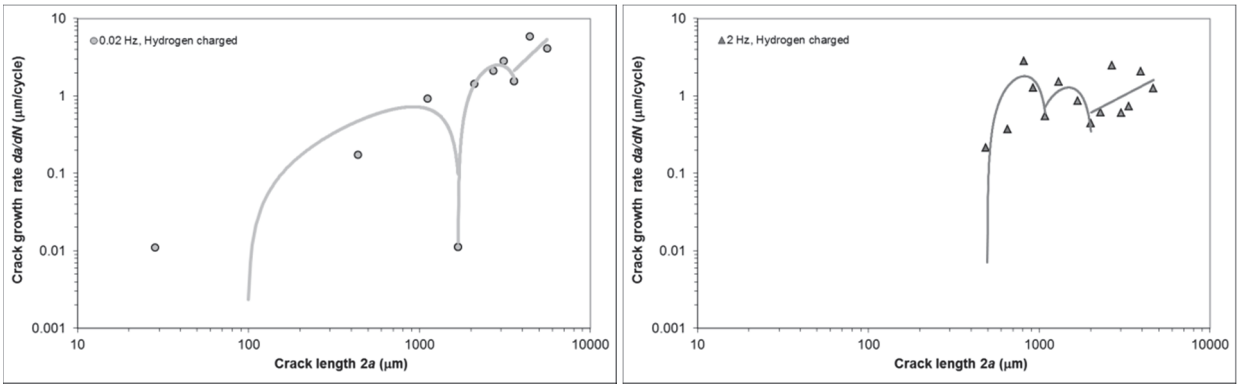

a) b)

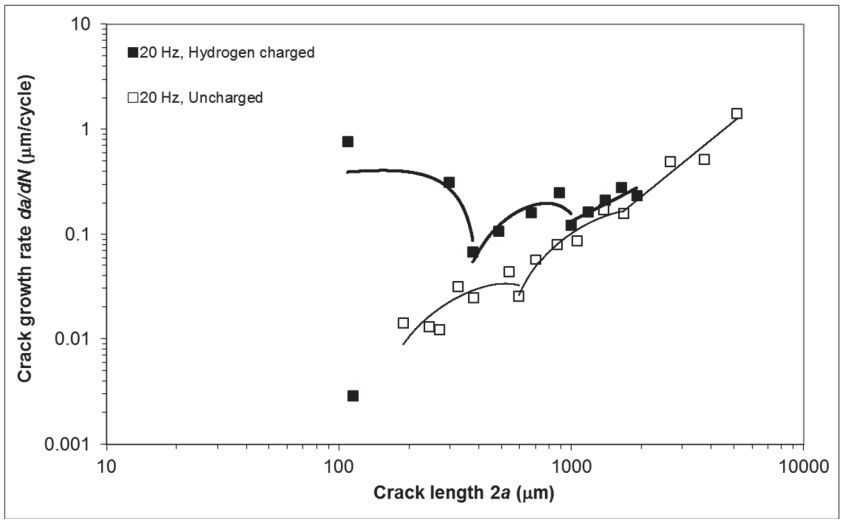

c)

Fig. 4 Presentation "Crack growth rate *da/dN* - Crack length, 2*a"* at different frequencies: a) 0.2 Hz; b) 2 Hz; c) comparison between hydrogen-charged and uncharged specimens tested at 20 Hz

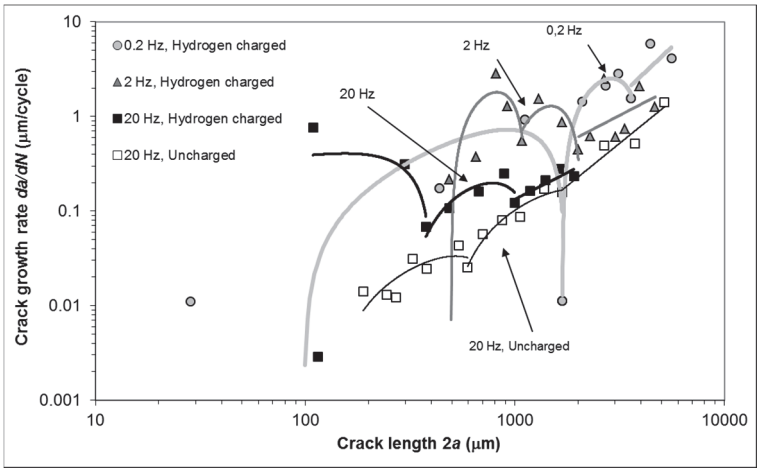

Fig. 5 Comparison between proposed model presentations for different frequencies

CONCLUSIONS

For investigated steel the obtained fatigue data are presented in plots “Crack length - Number of cycles” and “Fatigue crack growth rate - Crack length”. Mathematical modelling was done and showed (qualitatively) the same double-parabolic-linear-curve presentation for investigated steel in this work, which makes possible the prognostication of fatigue behaviour under different loading conditions. Another important point is that crack growth rate increases with decreasing of test frequency. The adequacy of presented models is checked and proved by comparison of experimental fatigue lifetimes and those calculated by the models. The error which is obtained in all cases is less than 10 percent.

ACKNOWLEDGEMENTS

Autors are grateful for the financial help of Project BG051PO001-3.3.06-0038 funded by OP Human Resources Development 2007-2013 of EU Structural Funds.

REFERENCES

[1] MURAKAMI, Y. The effect of hydrogen on fatigue properties of metals used for fuel cell system. *Int. J. Fracture*, 138, 1-4, 2006, 167-195.

[2] MURAKAMI, Y., MATSUOKA, S. Effect of hydrogen on fatigue crack growth of metals. *Eng. Frac. Mech.*, 77, 2010, 1926-1940.

[3] KANEZAKI, T., NARAZAKI, C., MINE, Y., MATSUOKA, S., MURAKAMI, Y. Effects of hydrogen on fatigue crack growth behavior of austenitic stainless steels. *Int. J. Hydrogen Energy*, 33, 2008, 2604-2619.

[4] YORDANOVA, R., ANGELOVA, D. *Plastic Deformation and Fracture of Metals. Physical Basis and Technological Descriptions. Methods for Mechanical Testing.* Textbook for laboratory seminars and experimental work, Sofia, Bulgaria: University of Chemical Technology and Metallurgy, 2010, 284.

[5] YORDANOVA, R. *Modeling of fracture process in a low-carbon 09Mn2 steel on the bases of short fatigue crack growth experiments. Comparative analyses on the fatigue behaviour of other steels*. Sofia, Bulgaria, Univercity of Chemical Technology and Metallurgy, PhD Thesis, 2003, 265.

[6] ANGELOVA, D., YORDANOVA, R. Investigation and Modeling of Bending Fatigue Behavior of a Low Carbon Steel. II. Mathematical Description and Analyses. In: Proc. *The 18th European Conference on Fracture (ECF18) “Fracture of Materials and Structures from Micro to Macro Scale”.* August/September, Dresden, Germany, 2010, [CD-ROM].

[7] MILLER K. J. *Metal Fatigue - Past, Current and Future*. London: Proc. Inst. Mech. Engrs, 1991.

[8] SURESH S. *Fatigue of Materials*. Cambridge Univ. Press, 1998.